Atourki, L.; Vega-Fleitas, E.; Marí, B.; Mollar García, MA.; Ahsaine, H.; Bouabid, K.; Ihlal, A. (2016). MAPbI2.9-xBrxCl0.1 hybrid halide perovskites: Shedding light on the effect of chloride and bromide ions on structural and photoluminescence properties. Applied Surface Science. 390:744-750. doi:10.1016/j.apsusc.2016.08.176

Atourki, L., Vega-Fleitas, Erica, Marí, B., Mollar García, Miguel Alfonso, Ahsaine, H.A., Bouabid, K., Ihlal, A. Applied Surface Science, 390, 0, 744-750 (2016). DOI: 10.1016/j.apsusc.2016.08.176

$MAPbI_{3-x-0.1}Br_xCl_{0.1}$ hybrid halide perovskites: Shedding light on the effect of chloride and bromide ions on structural and photoluminescence properties.

Lahoucine Atourki[*1], Erika Vega[2], Bernabé Marí[2], Miguel Mollar[2], Hassan Ait Ahsaine[3], Khalid Bouabid[1] and Ahmed Ihlal[1]

[1]Materials and Renewable Energy Laboratory, Faculty of Science, Ibn Zohr University, Agadir, Morocco

[2]Instituto de Diseño y Fabricación (IDF), Universitat Politècnica de València, València, Spain

[3]Laboratoire Matériaux et environnement LME, Faculté des Sciences d'Agadir, Université Ibn Zohr, Agadir, Morocco

Corresponding author: lahoucine.atourki@edu.uiz.ac.ma

Abstract

The optical and structural properties of $CH_3NH_3PbI_3$ can be adjusted by introducing other extrinsic ions such as chloride and bromide. In this work, mixed bromide iodide lead perovskites with a 10% fraction of chloride were prepared from methylamine, lead nitrate and the corresponding hydro acid (X=I, Br, Cl). They were then deposited as thin films on ITO substrate by the spin coating process. Thin film perovskites were then characterized by X-Ray Diffraction (XRD), Scanning Electron Microscopy (SEM), UV-Vis optical spectrometry and Photoluminescence analysis (PL). This work highlights the effect of bromide and chloride incorporation on different properties of perovskite thin film. The Pawley fit method indicates the formation of the iodide halide $MAPbI_3$ Pm-3m cubic phase for x= 0 and the tetragonal P4/mmm phase for $x \geq 0.3$. All deposited films showed a strong absorbance in the UV-Vis range. The band gap values were estimated from absorbance measurements. It was found that the onset of the absorption edge for $MAPbI_{3-x}Br_{x-0.1}$:10% Cl thin film perovskites ranges between 1.60 and 1.80 eV. PL emission energies of the mixed halide perovskite displayed intermediate values from 730 nm ($MAPbI_{2.2}Br_{0.7}Cl_{0.1}$) to 770 nm ($MAPbI_{2.6}Br_{0.3}Cl_{0.1}$).

Keywords: Pawley refinement, photoluminescence; gap energy tuning; chemical composition, thin film Perovskites, mixed bromide iodide lead perovskites.

1. Introduction

During the last recent years, methylammonium lead halide perovskites ($CH_3NH_3PbX_3$, X=halogen; CH_3NH_3: MA) and their mixed-halide crystals have been one of the most widely investigated optoelectronic materials by researchers in many different areas **[1]**. Perovskite materials exhibit a variety of interesting physical properties such as: high photoluminescence quantum efficiencies, long carrier lifetimes, very strong optical absorption, a low band gap around 1.4 eV **[1-4]** along with low-cost solution processability **[5]**. Perovskite materials are being widely used for many applications such as solar cell **[6]** light emitting diodes (LED) **[7, 8],** the water splitting reaction and the degradation of organic dyes **[9, 10].**

Although perovskite materials were synthesized for the first time in 1980 **[11]**, numerous publications have focused on growth and characterization of mixed lead halide perovskites. Particularly, $CH_3NH_3PbI_{3-x}Br_x$ has been reported to be an excellent absorber showing high power conversion efficiency and long stability compared to $MAPbI_3$ **[12, 13]**. In addition, $CH_3NH_3PbI_{3-x}Cl_x$ has recently been found to exhibit a longer carrier diffusion length compared with that of $CH_3NH_3PbI_3$ (~100 nm), and device performance has consequently been increased dramatically **[3, 14, 15]**

Due to the large difference between the ionic radii of Cl and I as well as the limited solubility of the chlorine containing precursors in dimethylformamide **[3, 16].** In this work, we focused on the preparation of solution processed mixed bromide iodide lead perovskites $MAPbI_{2.9-x}Br_xCl_{0.1}$ with a small fraction of chloride. We present a study on their structural and optical properties in order to better understand their properties and optimize their chemical composition to meet the requirement of different applications.

2. Experimental Procedure

$MAPbI_3$, $MAPbBr_3$ and $MAPbCl_3$ powders were first synthesized by reacting 0.30 mol of hydrohalide acid HX (X=I, Br, Cl) (in water, Sigma Aldrich), 0.30 mol of CH_3NH_2 (33% in methanol, Sigma Aldrich), and 0.030 mol of $Pb(NO_3)_2$ (in 50mL of distilled water, Sigma Aldrich) in a round-bottomed flask at 0°C for 2 h with stirring. The crystalline perovskite powders precipitate, i.e. ($MAPbI_3$ with black colour and $MAPbBr_3$ with orange colour). The remaining solution was then left to cool and filtered. The obtained powders were washed with

absolute ethanol and diethyl ether several times then they were dried under vacuum. All materials were purchased from either Sigma-Aldrich or Alfa Aesar and used as received.

The precursor solutions were prepared by dissolving $MAPbI_3$ and $MAPbBr_3$ powders at 45% wt dimethylformamide (DMF-Sigma Aldrich) solution and $MAPbCl_3$ at dimethyl sulfoxide (DMSO - Sigma Aldrich) 45%. The mixed perovskite solutions were prepared by varying the iodide /bromide amounts. The mixed solutions were stirred for 3 hours to insure the homogeneity of the solution. Thin film perovskites were then produced by spin coating at a speed of 4000 rpm for 30 seconds. Finally, the samples were annealed for 1 hour at 100°C and kept in vacuum to avoid their degradation.

The diffractograms of the perovskite films were measured by an X-ray diffractometer **(**RIGAKU Ultima IV in the Bragg-Bretano configuration using Cu K-alpha radiation (**λ**= 1.54060 Å). The surface morphology of the perovskite films was observed by an environmental scanning electron microscope FESEM (Quanta 200 − FEI). The absorption spectra of perovskite films were measured at room temperature using spectrometer Ocean Optics HR4000 spectrometer equipped with a Si-CCD detector. An integrating sphere was used to collect specular and diffuse transmittance. Photoluminescence (PL) was measured by an He-Cd (325 nm) laser and a spectrometer with a Hamamatsu back-thinned Si-CCD detector.

3. Results and Discussion

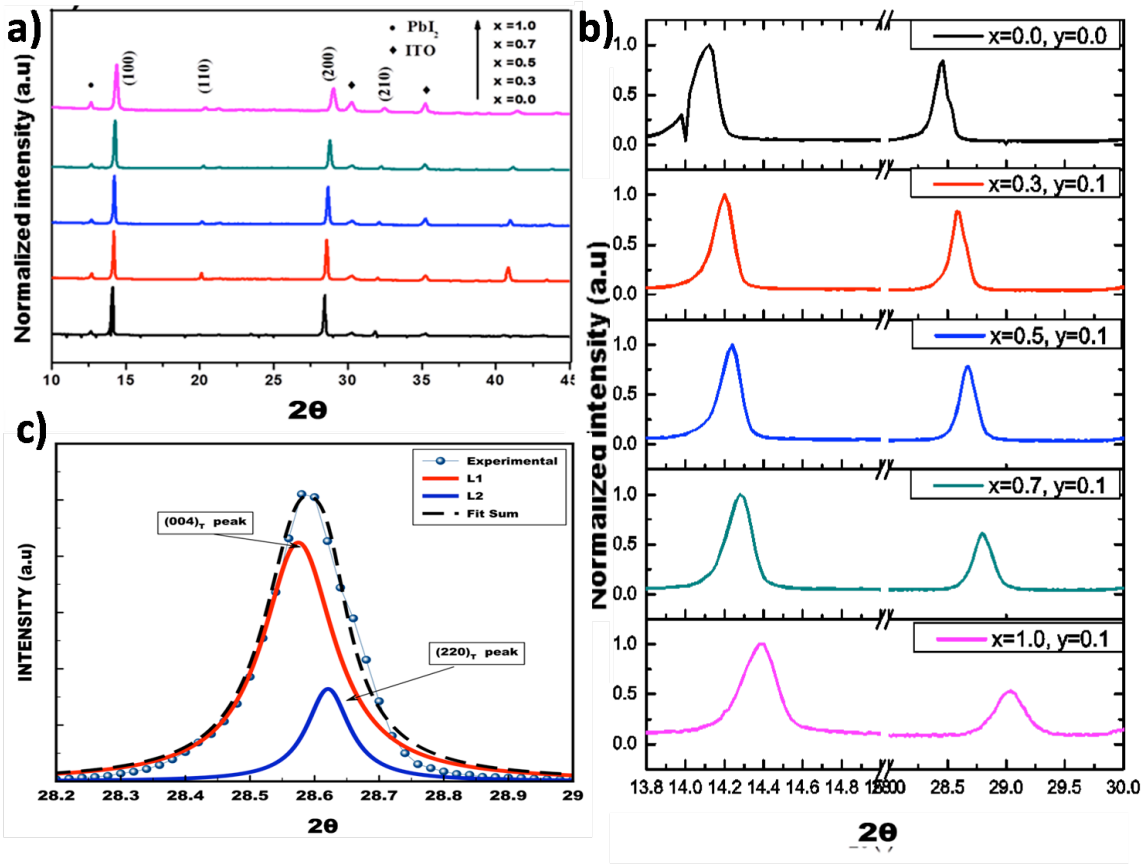

Figure 1 a) XRD patterns of $MAPbI_{3-x}Br_{x-0.1}$:10%Cl with x=0, 0.3, 0.5, 0.7 and 1.0; **b)** XRD patterns of $MAPbI_{3-x}Br_{x-0.1}$:10%Cl with different x values, magnified in the region of (2θ = 13.5°- 14.5°) and (2θ = 28.5°- 30.0°). **c)** Deconvolution of the peak at 28.5° in two tetragonal peaks (c)

Figure 1a shows the X-Ray diffractograms for $MAPbI_{2.9-x}Br_{x-0.1}Cl_{0.1}$ with different bromide fractions. The two strongest intensities are centered at 14.0° and 28.0°. Those peaks are assigned to the crystal planes of the tetragonal lattice of the mixed halide perovskite, indicating that the tetragonal perovskite structure is formed **[17]**. The peak located at around 12.6° is assigned to PbI_2 **[18]**. No other impurity peaks were detected**.**

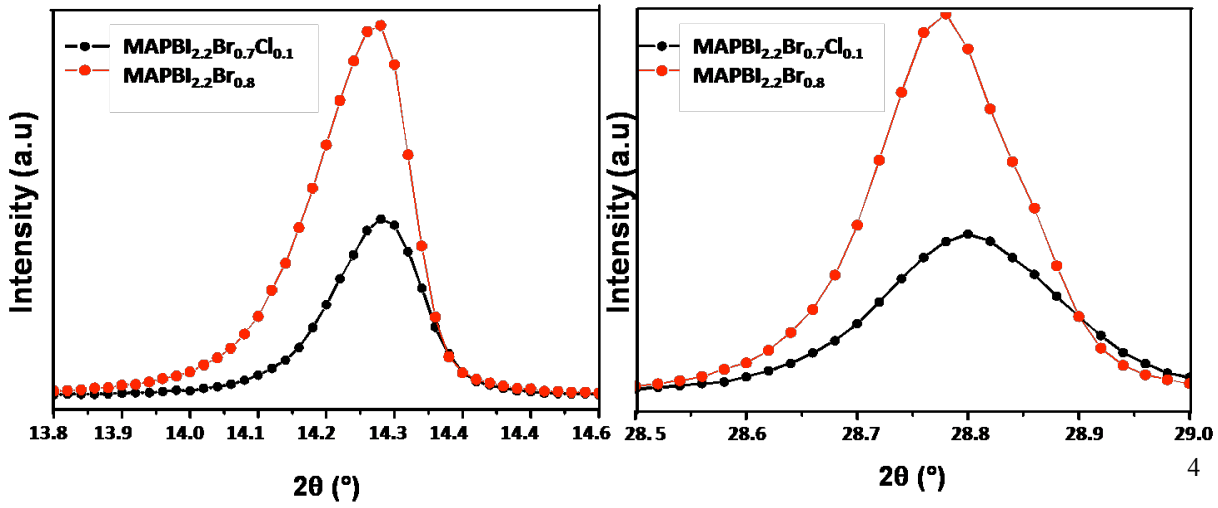

Figure 2. XRD patterns of $MAPb_{3-x}Br_x$ (x=0.2 & 0.4) with and without a 10% of chloride magnified in the region of (2θ = 13.8°- 14.6°) and (2θ = 28.3°- 29.0°).

Figure 1b shows the XRD patterns of $MAPbI_{2.9-x}Br_xCl_{0.1}$, with different bromide fractions, magnified in the region of (2θ = 13.5°- 14.5°) and (2θ = 28.5°- 30.0°). The position of the two peaks shifts to higher angles when the average fraction of bromide and chloride introduced into the thin film increases, which is due to the decrease of the lattice parameter resulting from the difference in the ionic radius of Cl^- (1.81A), Br^- (1.96A) and I^- (2.2A) **[9].** The shift in the 2θ position and the absence of a secondary phase confirm the formation of single-phase crystals with a mixed halide lattice **[19-22]**.

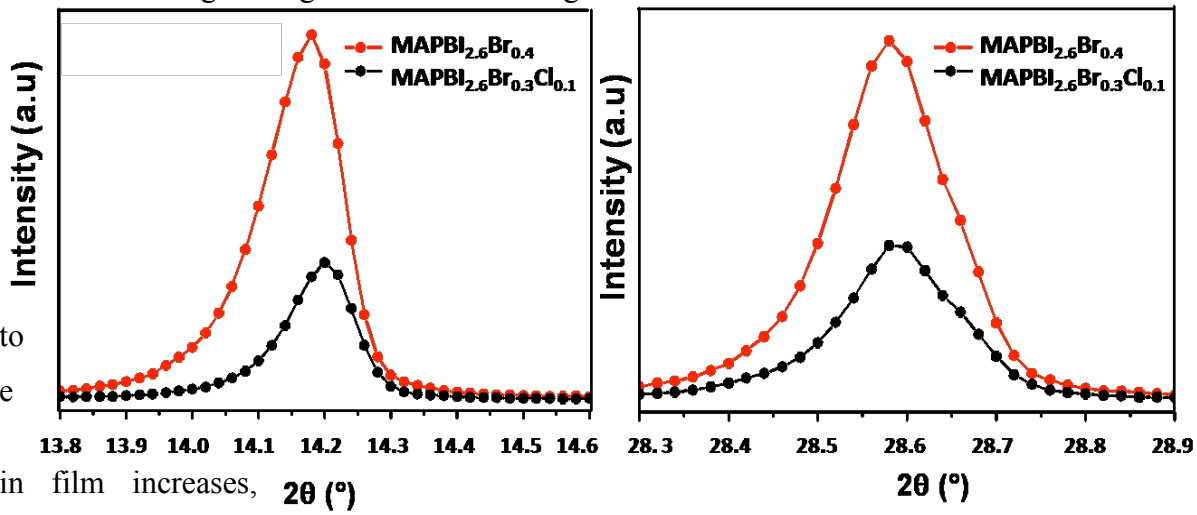

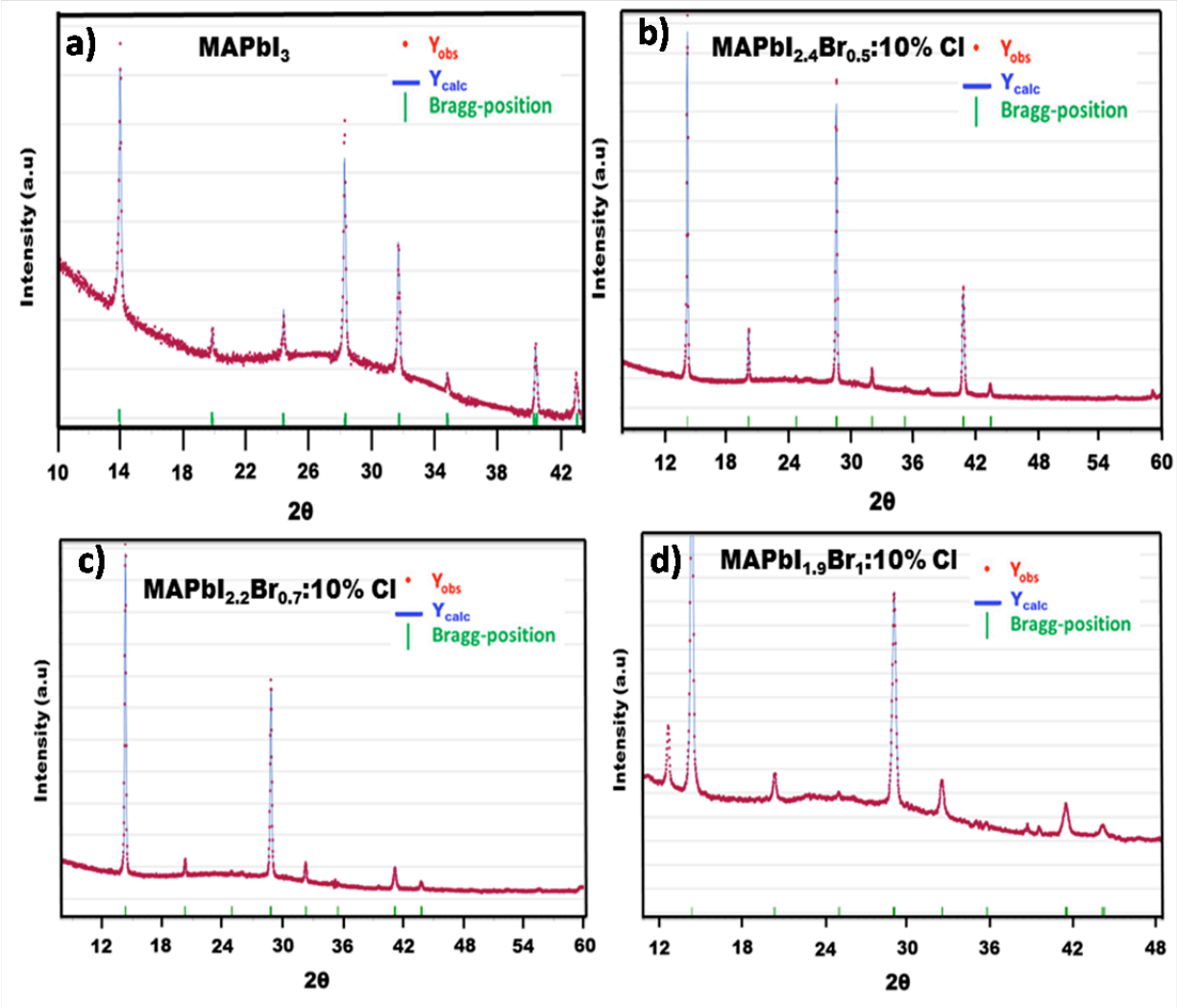

Figure 3. Pawley fit of the synthesized: **a)** $MAPbI_3$, **b)** $MAPbI_{2.4}Br_{0.5}Cl_{0.1}$, **c)** $MAPbI_{2.2}Br_{0.7}Cl_{0.1}$ and **d)** $MAPbI_{1.9}Br_{0.1}Cl_{0.1}$.

To have more insight into the chloride incorporation, we compared the XRD patterns of the $MAPbI_{3-x}Br_x$ (x=0.2, 0.4) with and without a 10% of chloride. The results are shown in Figure. 2. With the addition of 10% of chloride, we observe a slight shift toward higher angles of the peaks (100) and (200), located at 2θ ~ 14.2 and 2θ ~ 28.3, respectively. This might be due to the stresses in crystal lattice caused by interstitial vacancies, which are created by the introduction of the 10% chloride. However, it is unclear whether Cl occupied an interstitial position into $MAPb_{3-x}Br_x$ crystal or substitute Br at the surface of the crystal.

The Pawley refinement method was performed to fit the peak profiles, indicating:

- For x = 0, the formation of the iodide halide $MAPbI_3$ Pm-3m cubic phase.
- For x ≥ 0.3, the formations of the tetragonal P4/mmm phase.

Figure 3 shows the Pawley fit of the synthesized samples. ITO peaks were excluded from the diffraction; the factors Rp and Rwp were used as numerical criteria to evaluate the fitting quality of the simulated to experimental data.

Some peaks in the cubic-tetragonal region appeared broader, the existence of this double peak with high FWHM values, comes from the fact that the planes (00*l*) and (*hk*0) are related to *c* and *a*=*b* axes **[13]**. Indeed, in **Figure 1 (c)** the XRD peak at ~28.5° of the $MAPbI_{2.6}Br_{0.3}Cl_{0.1}$ can be decomposed to two Lorentzian tetragonal peaks, the reflections $(004)_T$ (Red L1) and $(220)_T$ (Blue L2), which explains the formation of the tetragonal P4/mmm phase up to the open range $0.3 \leq x$ of the bromide content. New defect centers were created in the $MAPbI_3$ host material by doping with chloride and bromide

The refined cell parameters through Pawley fit, for the synthesized thin films, are reported in **Table 1**. It is shown that the lattice parameters decrease with the increase of the Br and Cl. Content.

Table 1: Refinement factors and refined cell parameters using the Pawley fit method.

Sample id.	**a = b (Å)**	**c (Å)**	**R_p**	**R_{wp}**
$MAPbI_3$	6.3023(3)	6.3023(3)	2.23%	3.23%
$MAPbI_{2.6}Br_{0.3}Cl_{0.1}$	4.4189(2)	6.2471(3)	3.43%	5.42%
$MAPbI_{2.4}Br_{0.5}Cl_{0.1}$	4.4033(2)	6.2247(9)	3.17%	4.92%
$MAPbI_{2.2}Br_{0.7}Cl_{0.1}$	4.3814(2)	6.1900(4)	3.03%	4.32%
$MAPbI_{1.9}Br_1Cl_{0.1}$	4.3494(3)	6.1384(5)	1.99%	2.81%

SEM was further used to investigate the film morphologies of $MAPI_{2.9-x}Br_xCl_{0.1}$. **Figure 4** shows that the perovskite films with and without chloride exhibit a similar crystal texture and film conformity. The films are homogenous and the crystalline particles are aggregated into larger crystals with a larger dimension. In addition, SEM analysis shows a morphology with good coverage and no apparent crystal orientation. The presence of uncovered areas among the perovskite aggregates may have originated from the evaporation of the solvent used during the film preparation. We found that the presence of 10% of chloride increases the number of voids and uncovered areas. Indeed, chloride incorporation was seen to affect the film morphology. Indeed, many authors have reported the enhancement of the film reconstruction and mass transport due to chloride incorporation **[23, 24**]. In addition, different studies reported that chloride slows down the nucleation and growth of perovskite crystals, leading to better quality films **[25, 26].**

To check the variation of optical properties in thin film perovskites, we measured the UV–visible absorption spectra of $MAPbI_{2.9-x}Br_{x-0.1}Cl_{0.1}$ perovskites, which is shown in **Figure 5 a.** The band gap was estimated from the onset of the absorption edge, which increased as the fraction of bromide increased, i.e. - perovskite colours change from brown to red region. Band gap energy values were ~1.80 eV for $MAPbI_{1.9}Br_{1.0}Cl_{0.1}$ and 1.61 eV for $MAPbI_{2.6}Br_{0.3}Cl_{0.1}$. This change of the band gap energy is due to the structural distortion caused by the change in stress of Pb-I bonds after the Br and Cl inclusion **[27].**

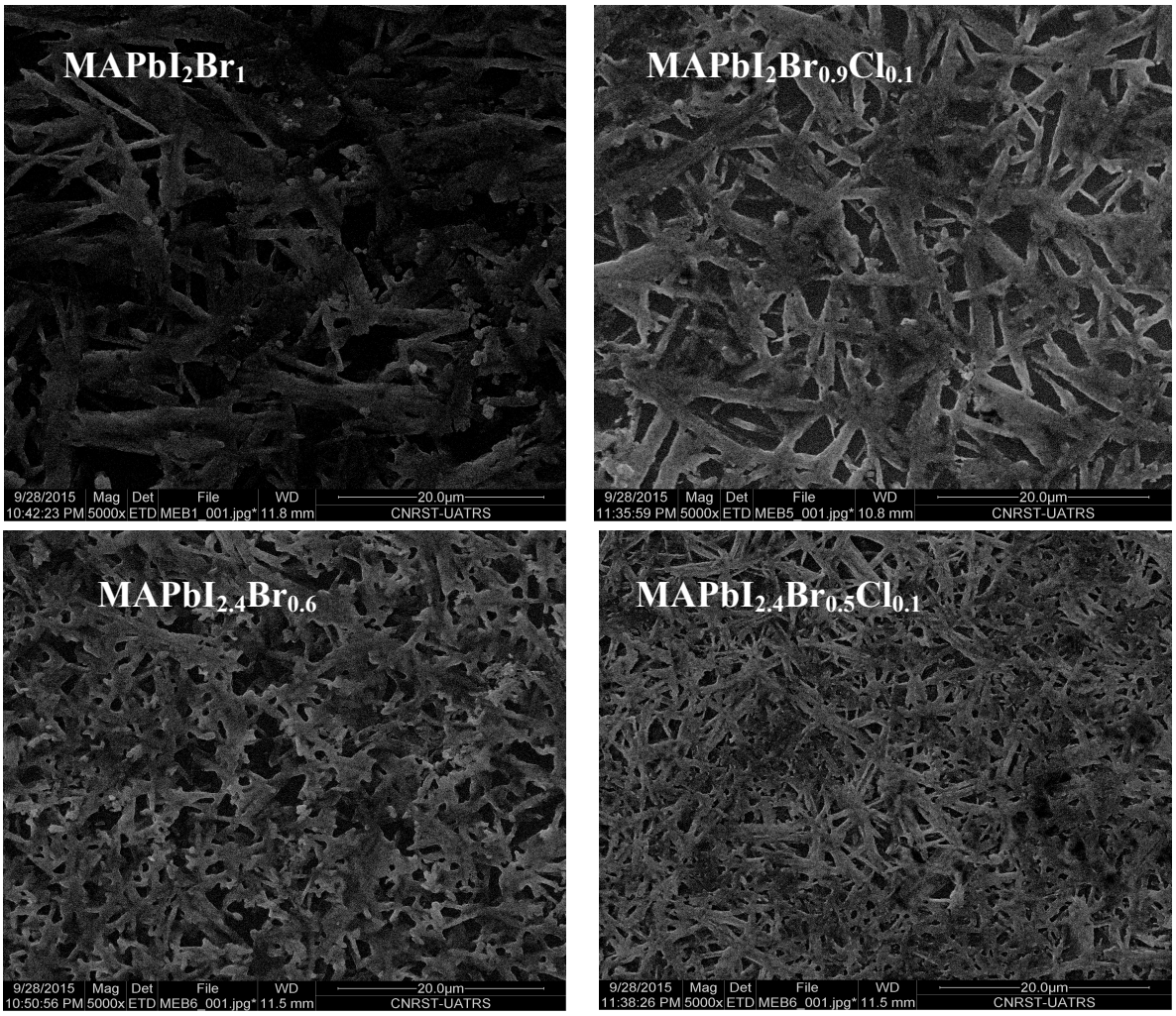

Figure 4. Top view SEM image of $MAPbI_2Br_1$, $MAPbI_2Br_{0.9}Cl_{0.1}$, $MAPbI_{2.4}Br_{0.6}$ and $MAPbI_{2.4}Br_{0.5}Cl_{0.1}$ deposited on ITO substrate using the spin coating process.

We further investigated the effect of chloride incorporation into the $MAPbI_{3-x}Br_x$ structure by measuring the UV–visible absorption of mixed hybrid halide perovskites with and without 10% of chloride. The results are illustrated in **Figure 5.b** and in **Table 2**. The results revealed

that the introduction of a very small fraction of chloride to $MAPI_{3-x}Br_x$ changes the band gap value slightly, which implies the formation of an increasing amount of vacancies due to the presence of chloride/bromide in the thin films, which would involve additional energy levels in the band gap. Usually, both bromide and chloride addition shifts the PL to higher energy values **[19, 28, 29]**. Nevertheless, in our case the introduction of 10% of chloride shifts the band gap slightly toward lower energies due to the lower quantity of bromide in the $MAPb_{2.4}Br_{0.3}Cl_{0.1}$ compared to $MAPb_{2.4}Br_{0.6}$.

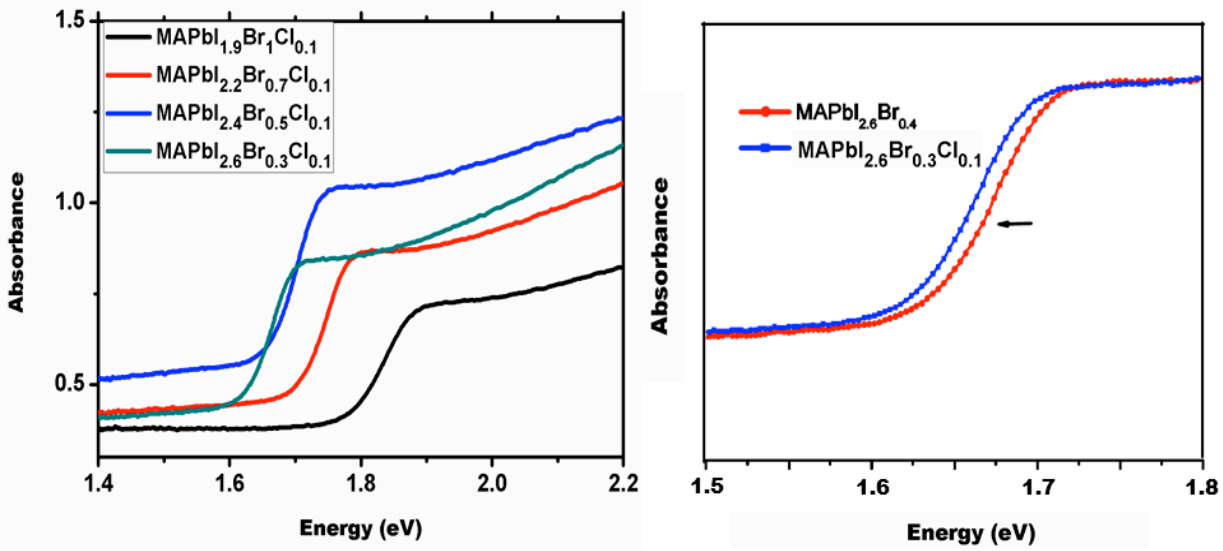

Figure 5.a) UV-Vis absorption spectra of $MAPbI_{2.9-x}Br_{x-0.1}Cl_{0.1}$ with (x=0, 0.3, 0.5, 0.7, 1.0). **b)** Comparison UV-Vis absorption spectra of $MAPbI_{2.6}Br_{0.4}$ and $MAPbI_{2.6}Br_{0.3}$:10%Cl.

Table 2: Band gap of $MAPI_{3-x}Br_x$ compared with $MAPbI_{2.9-x}Br_{x-0.1}Cl_{0.1}$ in case of x=0.8, 0.6, 0.4

	$MAPbI_{2.2}Br_{0.8}$	$MAPbI_{2.2}Br_{0.7}Cl_{0.1}$	$MAPbI_{2.4}Br_{0.6}$	$MAPbI_{2.4}Br_{0.5}Cl_{0.1}$	$MAPbI_{2.6}Br_{0.4}$	$MAPbI_{2.6}Br_{0.3}Cl_{0.1}$
Band gap (eV)	**1.71**	**1.70**	**1.66**	**1.64**	**1.63**	**1.61**

Figure 6 displays the photoluminescence measurement (PL) recorded on mixed halide perovskite thin films at room temperature. The position of the maximum of the photoluminescence emission is found to shift to a lower wavelength as the fraction of bromide increases. This evolution tendency is similar to the one observed in the UV-Vis absorption analysis. The Gaussian emissions are essentially bromide dependent, thus, the room

photoluminescence emission can be tuned from ~730 to 770 nm by adding a small fraction of bromide. In **Figure 6.b** we observed that the $MAPbI_{2.6}Br_{0.4}$ presented a higher blue shift than the $MAPb_{2.6}Br_{0.3}$:10%Cl which shows a slight shift toward higher energies. This shifting tendency was also observed in the X-ray patterns of the synthesized films. Therefore, the introduction of 10% chloride in the halide lattice band gap level diminishes the blue shifting meaning that even small quantity of chloride can affect the thin films emissions. The observed trend in the optical and luminescence spectra is in agreement with the X-ray diffraction data of the mixed halide perovskites. Further analyses are needed in order to investigate whether Cl substitutes Br or it just occupied interstitial sites.

The narrower emission bands, with a full width at half maximum (FWHM) of 40 nm, of the perovskite halide thin films are due to the amplified spontaneous emissions **[30, 31]**. We believe that doping with chloride ions can enhance the near infrared emissions and the films can be potential candidates for near-infrared light emitting diodes (NIR-LED). In addition, recently it has been confirmed that the role of chloride spectator ions can lead to high quality films with exceptional smoothness **[32-34].**

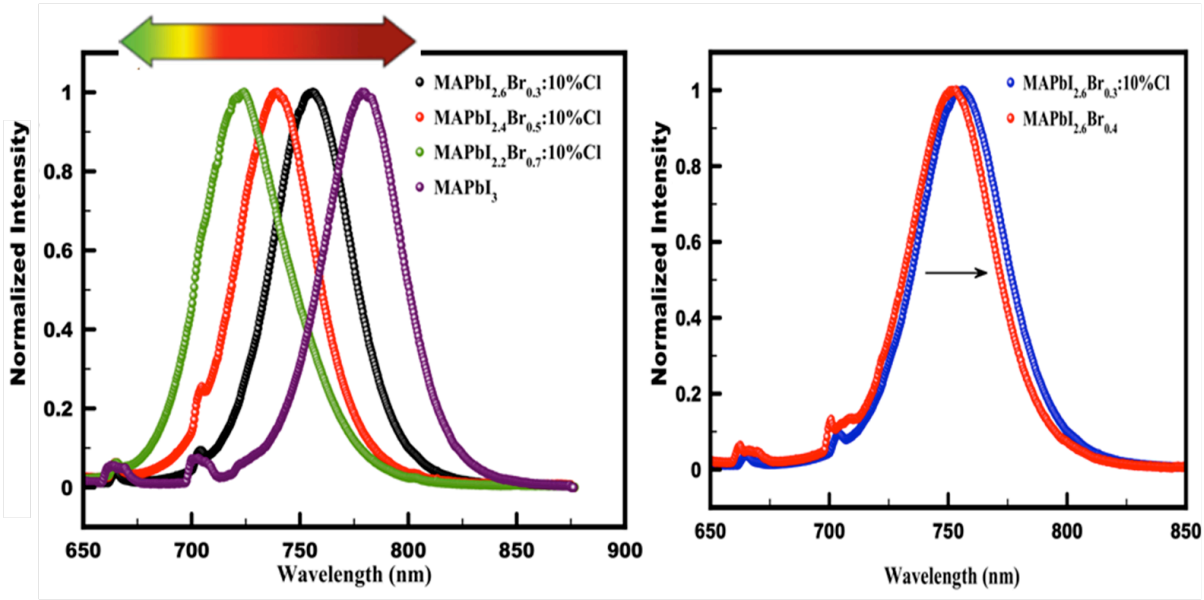

Figure 6.a) Room photoluminescence spectra (PL) for $MAPbI_3$ and $MAPbI_{2.9-x}Br_{x-0.1}Cl_{0.1}$ with x= 0.3, 0.5, 0.7. **b)** Comparison between the emissions of $MAPbI_{2.6}Br_{0.4}$ and $MAPbI_{2.6}Br_{0.3}$:10%Cl **.**

4. Conclusion

In this work, the structural and optical properties of $MAPbI_{2.9-x}Br_xCl_{0.1}$ perovskite thin films prepared by the single step spin-coating process have been investigated. The films were homogenous and adherent to the substrate with a strong absorbance in the UV-Vis range. The Pawley fit method indicates the formation of the iodide halide $MAPbI_3$ Pm-3m cubic phase for x= 0 and tetragonal P4/mmm phase for $x \geq 0.3$. The band gap energy of thin film perovskite was inferred from absorbance spectral measurements. It was found that the onset of the absorption edge for $MAPbI_{2.9-x}Br_xCl_{0.1}$ thin film perovskites ranges from 1.60 to 1.80 eV in the composition range of $0.3 \leq x \leq 1$. PL emission energies for mixed halide perovskites are located in intermediate values between ~730 nm ($MAPbI_{2.2}Br_{0.7}Cl_{0.1}$) and 770 nm ($MAPbI_{2.6}Br_{0.3}Cl_{0.1}$).

Acknowledgments

This work was supported by Ministerio de Economía y Competitividad (ENE2013-46624-C4-4-R) and Generalitat Valenciana (Prometeus 2014/044).

References

[1] Z. Xiao, Y. Yuan, Q. Wang, Y. Shao, Y. Bai, Y. Deng, Q. Dong, M. Hu, C. Bi, J. Huang, Mater. Sci. Eng. R, 2016, 101, 1–38

[2] H.-S. Kim, C.-R.Lee, J.-H.Im, K.-B.Lee,T. Moehl, A. Marchioro, S.-J. Moon, R. Humphry-Baker, J.-H.Yum, J. E. Moser, M. Gratzel, N.-G. Park, Sci. Rep., 2012, 2, 1–7.

[3] S.D. Stranks, G.E. Eperon1, G. Grancini, C. Menelaou, M.J. P. Alcocer, T. Leijtens, L. M. Herz, A. Petrozza, H.J. Snaith, Science, 2013, 342, 341-344.

[4] A. Kojima, K. Teshima, Y. Shirai, T. Miyasaka, J. Am. Chem. Soc., 2009, 131, 6050–6051.

[5] J. You, Z. Hong, Y. Yang, Q. Chen, M. Cai, T.-B. Song, et al., ACS Nano.,2014, 8, 1674–1680.

[6] M. Bag, Z. Jiang, L.A. Renna, S. Pyo Jeong, V.M. Rotello, D. Venkataraman, Mater. Lett, 2016, 164, 472–475.

[7] Z.-K. Tan, R. S. Moghaddam, M.L. Lai, P. Docampo, R. Higler, F. Deschler, M. Price, A. Sadhanala, L.M. Pazos, D. Credgington, F. Hanusch, T. Bein, H.J. Snaith , R. H. Friend, Nat. Nanotechnol.,2014, 9, 687–692.

[8] G. Li, Z.-K. Tan, D. Di, Ma.L. Lai, L. Jiang, J. H.-W. Lim, R. H. Friend, Neil C. Greenham, Nano. lett., 2015, 15, 2640-2644.

[9] M. M. Lee, J. Euscher, T. Miyasaka, T. N. Murakami and H. J. Snaith, Science,2012, 338, 643–647.

[10] Z. X. Wei, Y. Wang, J. P. Liu, C. M. Xiao, W.W. Zeng, Mater. Chem. Phys., 2012, 136, 755–761.

[11] D. Weber, Z. Naturforsch. B, 1978, 33, 862–865.

[12] J. He, T. Chen, J. Mater. Chem. A, 2015, 3, 18514-18520.

[13] L. Atourki, E. Vega, B. Marí, M. Mollar, H. Ait Ahsaine, K. Bouabid, A. Ihlal, Appl. Surf. Sci., 2016, 371, 112–117.

[14] G.Xing, N.Mathews, S. Sun, S.S. Lim, Y.M. Lam, M. Grätzel, S.Mhaisalkar, T.C. Sum, Science, 2013, 342, 344–347.

[15] Y. Tidhar, E. Edri, H. Weissman, D. Zohar, G. Hodes, D. Cahen, B. Rybtchinski, S. Kirmayer, J. Am. Chem. Soc. 2014, 136, 13249–1325.

[16] Y. Zhou, M. Yang, W. Wu, A. L. Vasiliev, K. Zhu, N. P. Padture, J. Mater. Chem. A , 2015, 3, 8178.

[17] T. Baikie, Y. Fang, J. M. Kadro, M. Schreyer, F. Wei, S. G. Mhaisalkar, M. Graetzel, T. J. White, J. Mater.Chem. A, 2013, 1, 5628–5641.

[18] D Liu, T.L. Kelly, Nat. Photon., 2014, 8, 133–138.

[19] S. Pathak, N. Sakai, F.W.R. Rivarola, S.D Stranks, J. Liu, G. Eperon, C. Ducati, K. Wojciechowski, J.T. Griffiths, A.A. Haghighirad, A. Pellaroque, R.H. Friend, H.J. Snaith, Chem. Mater., 2015, 27, 8066–8075.

[20] G.E. Eperon, S.D. Stranks, C. Menelaou, M.B. Johnston, L.M. Herz, H. Snaith, Energy Environ. Sci., 2014, 7, 1764–1769.

[21] G.C. Papavassiliou, G. Pagona, N. Karousis, G.A. Mousdis, L. Koutselas, A. Vassilakopoulou, J. Mater. Chem., 2012, 22, 8271–8280.

[22] J.H. Noh, S.H. Im, J.H. Heo, T.N. Mandal, S.Il. Seok, Nano Lett., 13, 2013, 13, 1764–1769.

[23] H.Yu, F. Wang, F. Xie, W. Li, J. Chen, N. Zhao, Adv. Funct. Mater., 2014, 24, 7102-7108.

[24] Q. Chen, H. Zhou, Y. Fang, A.Z. Stieg, T.-B. Song, H.-H. Wang, X. Xu, Y. Liu, S. Lu, J. You, P. Sun, J. McKay, M. S. Goorsky, Y. Yang, Nat. Comm., 2014, 6, 7269.

[26] S.T. Williams, F. Zuo, C.-C. Chueh, C.-Y. Liao, P.-W. Liang, A. K.-YJen, ACS Nano., 2014, 08, 10640-10654

[27] Y. Zhao, K.J. Zhu, Phys. Chem. C, 2014, 118, 9412-9418.

[28] E. Mosconi, A. Amat, M.K. Nazeeruddin, M. Grätzel, F. De Angelis, J. Phys. Chem. C, 2013, 117, 13902–1391.

[29] E. Vega, M. Mollar, B. Marí, Physica Status Solidi C, 2016, 13, 30-34 .

[30] F. Deschler, M. Price, S. Pathak, L.E. Klintberg, D.-D. Jarausch, R. Higler, S. Hüttner, T. Leijtens, S.D. Stranks, H.J. Snaith, M. Atatüre, R.T. Phillips, R.H. Friend, J. Phys. Chem. Lett., 2014, 5, 1421–1426

[31] G. Xing, Nature Mater., 2014, 13, 476–480

[32] W. Zhang, M. Saliba, D.T. Moore, S.K. Pathak, M.T. Hörantner, T. Stergiopoulos, S.D. Stranks, G.E. Eperon, J.A. Alexander-Webber, A. Abate, A. Sadhanala, S. Yao, Y. Chen, R.H. Friend, L.A. Estroff, U. Wiesner, H.J. Snaith, Nature Commun., 2015, 6, 6142.

[33] D.T Moore, H. Sai, K.W. Tan, D.-M. Smilgies, W. Zhang, H.J. Snaith, U. Wiesner, L.A. Estroff, J. Am. Chem. Soc., 2015, 137, 2350–2358.

[34] A. Buin, P. Pietsch, J. Xu, O. Voznyy, A.H. Ip, R. Comin, E.H. Sargent, Nano. Lett., 2014, 6281–6286.